3D Visualization of Cardiac Tagged Magnetic Resonance Image data using Non-Uniform Rational B-Splines (NURBS)

Sudarshan Ramenahalli*
Electrical and Computer Engineering
Johns Hopkins University
Baltimore, MD, USA
sramena1@jhu.edu

Thomas S. Denney Jr.
Electrical and Computer Engineering
Auburn University
Auburn, AL, USA
dennets@auburn.edu

ABSTRACT

The paper demonstrates accurate, anatomically correct 3D visualization of left and right ventricles of the human heart from tagged magnetic resonance imaging data. Tagged MRI reveals 3D structural and motion information that is incorporated into the visualized models. We use Non-Uniform Rational B-Splines (NURBS) for our purpose, that allow non-uniform knot specification and weight specification of control points, an advantage over traditional uniform B-Splines. NURBS algorithms are numerically stable and fast. The myocardial models serve the purpose of (i)accurate visualization of tag planes and myocardial walls, (ii)checking tag tracking accuracy and registration errors, (iii)providing framework for 4D visualization and motion analysis, and (iv)obtaining accurate, memory efficient and compactly supported models of the heart in anatomical dimensions. We obtain excellent results on normal as well as pathological patient datasets.

Keywords

myocardial tagging, MRI, visualization, NURBS, surface lofting

1. INTRODUCTION

Myocardial tagging[15, 1] enabled non-invasive measurement of myocardial deformation. Magnetic resonance(MR) tagging is a technique in which myocardial tissue is magnetically saturated to create desired pattern planes that moves along with the underlying tissue. The patterned magnetic planes, created by application of special RF and gradient pulses, are called *tag planes*. The tag planes are orthogonal to the imaging plane. On the imaging plane, the projection of tag planes appear as *tag lines*, approximately 2 pixels wide

*Corresponding author

ICVGIP '10, December 12-15, 2010, Chennai, India

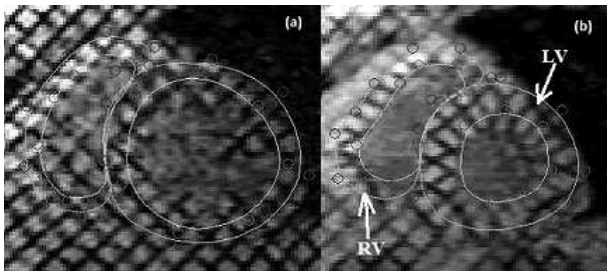

Figure 1: Tagged Short-Axis Image.(a)End-Diastole(b)End-Systole.[LV:Left-Ventricle,RV:Right-Ventricle]

[Fig.1]. On the short axis imaging plane, left ventricle(LV) appears like an annular ring whereas right ventricle(RV) has a complex shape and appears like a crescent.

The tag planes (lines) deform with the underlying myocardial tissue enabling visualization and quantification of deformation. In MR tagging, imaging plane is fixed throughout the cardiac cycle. Two important phases in cardiac cycle are:

- **End-Diastole(ED):** The left ventricle is filled with blood, completely relaxed and has highest volume in the entire cardiac cycle
- **End-Systole(ES):** The time instant at which, LV is completely compressed (least volume in the cardiac cycle).

As heart undergoes pseudo-cyclic contraction and relaxation, myocardial tissue and tag planes move in and out of the imaging plane. The out-of-plane motion of myocardium is not captured on the imaging plane; hence we need three mutually orthogonal sets of tag planes (short and long axis images) to fully reconstruct 3D motion of the myocardium.

We use Non-Uniform Rational B-Splines(NURBS) for the purpose of model construction and visualization. Tissue motion and deformation information, as revealed from moving myocardial boundaries and deforming tag lines, is extracted and incorporated into the NURBS models. A semi-automated algorithm is used for tag line tracking. The motivation to use NURBS over nonrational, uniform B-Splines is that NURBS allows specification on nonuniform knot spacing and assignment of weights to control points. This feature

of NURBS leads to less number of control points, increased accuracy and efficient storage with less memory. In addition, we can modify the degree and position of control points, a feature common to NURBS as well as B-Splines curves.

Our work focuses on building full 3D myocardial model incorporating information from myocardial contours as well as tag lines. We demonstrate applicability of this method to tagged MR dataset. However, the method is very versatile and can be applied to any type of imaging modality like CT, SPECT, PET etc, where a set of cross-sectional images are acquired. Deformation measurement is specific to tagged MR modality. Hence, when the method is applied to other modalities, we can only reconstruct the 3D bi-ventricular surface models.

In section 2, a brief survey of existing literature on myocardial model reconstruction from various modalities like MR, CT, Ultrasound imaging etc, is presented. Section 3 deals with mathematical concepts underlying NURBS. Section 4 details materials and methods used in the experiment and illustrates the efficacy of our algorithm with several examples. In section 5 we discuss the technical details of model reconstruction and conclude the paper in Section 6.

2. RELATED WORK

Initial approaches to left ventricular surface modeling used simple geometrical shapes like *truncated bullet*[2]. *Deformable superquadrics*[9] is another approach taken in the past. B-Spline and bi-cubic hermite surface patches have been used to reconstruct myocardial surfaces from cross sections[8, 7]. Shi et al,[12, 5] use *delaunay triangulation* to build myocardial surface model from a set of 2D contours obtained from cross-sectional images. The methods discussed so far, model the left ventricle only. Finite element methods[6] have been used to reconstruct biventricular myocardial models. Amini et al[11] used 4D coupled B-splines(B-Solid) to model the left ventricle and compute strain by incorporating tag data into the model. Tustison et al[13] have used NURBS based models for computation of strains. In their work, main purpose is deformation analysis and strain computation. The surfaces are coupled in their model where as in our model, none of the surfaces are coupled. Even though our work has been motivated by[13], the primary motivations of our work are, (i)fast, accurate and memory efficient visualization of tagged MRI data in anatomical dimensions, and (ii) aiding the image analyst in tracking of tag lines by visualizing tracking errors.

3. MATHEMATICAL PRELIMINARIES

NURBS curves are rational curves that are invariant under common geometric transformations like perspective and parallel projection. NURBS provides a unified framework for representation of analytic as well as free-form shapes. NURBS algorithms are fast and numerically stable making them ideal for fast, detailed and accurate visualization of complicated anatomical free-form shapes. In the next section, some fundamental properties of NURBS curves are detailed.

3.1 Definition and Properties of NURBS

A NURBS curve or surface is built on the basis of B-Splines, which are piecewise polynomial basis functions. A zero degree B-Spline basis function, $N_{i,0}(\overline{u})$ is defined as,

$$N_{i,0}(\overline{u}) = \begin{cases} 1 & \text{if } u_i \leq \overline{u} < u_{i+1} \\ 0 & \text{otherwise} \end{cases} \tag{1}$$

where $\{\overline{u}\}$ are parametric variables along which the curve is evaluated, $\mathbf{U} = \{u_0, u_1, ..., u_{m-1}, u_m\}$, a non-decreasing sequence(i.e.$u_i \leq u_{i+1}$) of real numbers is called the *knot vector* and u_i are called *knots*.

Any higher order basis functions can be computed using lower order basis functions using the relation,

$$N_{i,p}(\overline{u}) = \frac{\overline{u} - u_i}{u_{i+p} - u_i} N_{i,p-1}(\overline{u}) + \frac{u_{i+p+1} - \overline{u}}{u_{i+p+1} - u_{i+1}} N_{i+1,p-1}(u) \tag{2}$$

The above relation is the *Cox-de Boor recursion formula*[3]. A p-th degree NURBS curve is defined as,

$$\mathbf{C}(\overline{u}) = \frac{\sum_{i=0}^{n} N_{i,p}(\overline{u}) w_i \mathbf{P}_i}{\sum_{i=0}^{n} N_{i,p}(\overline{u}) wi} \qquad a \leq \overline{u} \leq b \tag{3}$$

where $\{\mathbf{P}_i\}$ are $n$control points, $\{w_i\}$ are weights, $\{N_{i,p}(\overline{u})\}$ are p-th degree B-Spline basis functions defined on the knot sequence, $\mathbf{U} = \{\underbrace{a, a, a}_{p+1}, u_{p+1}, \cdots, u_{m-p-1}, \underbrace{b, b, b}_{p+1}\}$. For computational simplicity, we set $a = 0; b = 1;$and $w_i > 0, \forall i$. Let,

$$R_{i,p}(\overline{u}) = \frac{N_{i,p}(\overline{u}) w_i}{\sum_{j=0}^{n} N_{j,p}(\overline{u}) w_j} \tag{4}$$

Then, we can rewrite (3) as,

$$\mathbf{C}(\overline{u}) = \sum_{i=0}^{n} R_{i,p}(\overline{u}) \mathbf{P}_i \tag{5}$$

where $\{R_{i,p}(\overline{u})\}$ are rational basis functions and have the following important properties:

- **Non-negativity:** $\{R_{i,p}(\overline{u})\} \geq 0, \qquad \forall i, p; u \in [0, 1]$
- **Partition of Unity:** $\sum_{i=0}^{n} R_{i,p}(\overline{u}) = 1 \qquad$ for all $u \in [0, 1]$
- **Local Support:** $R_{i,p}(\overline{u}) = 0 \qquad$ for all $\overline{u} \notin [u_i, u_{i+p+1})$. If a control point, $\mathbf{P}_i$ is moved OR weight, w_i is changed, only the portion of the curve on the interval $\overline{u} \in [u_i, u_{i+p+1}]$ is affected
- $\mathbf{C}(\overline{u})$ is C^{∞} continuous on any internal knot span and C^{p-k} continuous at a knot of multiplicity, k

In addition to the above listed excellent mathematical properties, weight modification allows us to control the shape of the curve within any desired knot span. Increasing the weight of a control point pulls the curve toward control polygon in that knot span[Fig.2].

Data like anatomical boundaries, tag lines etc, can be generated by a segmentation program, tag tracking or some similar external program. In order to build NURBS based anatomical models, we should first transform the set of points (object boundaries, surfaces etc) to its respective NURBS representation. We can obtain NURBS representation of a pointset by *interpolation* or *approximation*. More details on these techniques can be found in [10]. In the next section, we discuss an approximation technique used in our work.

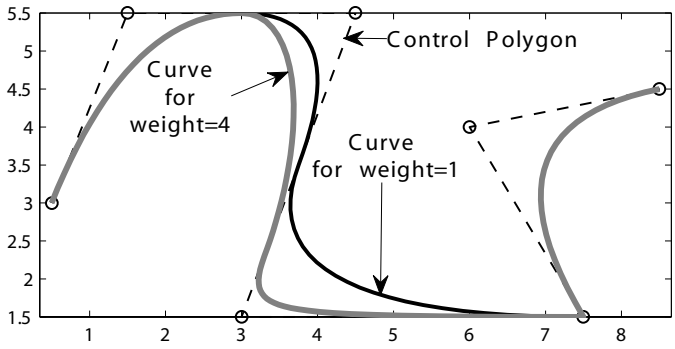

Figure 2: Effect of weight modification on NURBS curve

3.2 NURBS Curve Approximation Within a Specified Accuracy

Let $\{\mathbf{Q}_k\}$, for $k = 0, \cdots, m$ be the set of $\mathbf{m}$ data points to which a NURBS curve of degree, p and $n+1$ control points($m > n$) has to be fitted within a specified accuracy. The points, $\{\mathbf{Q}_k\}$ could be myocardial contours manually delineated or tag data points. NURBS curve fitting can be accomplished in three steps as follows:

3.2.1 Compute Curve Parameterization

The most widely used parameterization method that also serves our purpose is the *chord-length* parameterization. With $\{\mathbf{Q_k}\}$ as data points, let us define the total chord length, d as,

$$d = \sum_{k=1}^{m} \|\mathbf{Q}_k - \mathbf{Q}_{k-1}\|_2 \tag{6}$$

Let $\{\overline{u}_k\}$ for $k = 0, \cdots, m$ be the parametric points corresponding to the data points, $\{\mathbf{Q}_k\}$. We can compute $\{\overline{u}_k\}$ as,

$$\overline{u}_0 = 0 \qquad \overline{u}_m = 1 \tag{7}$$

$$\overline{u}_k = \overline{u}_{k+1} + \frac{\|\mathbf{Q}_k - \mathbf{Q}_{k-1}\|_2}{d} \quad \text{for } k = 1, \cdots, m-1 \tag{8}$$

3.2.2 Compute Knot Vector

Let $\mathbf{U} = \{u_0, u_1, ..., u_{r-1}, u_r\}$ be the knot vector that has to be computed. For best approximation results, the placement of knots $\{u_k\}$ should reflect the distribution of curve parameterization, $\{\overline{u}_k\}$.

For generating knots, let us define t to be a positive real number such that,

$$t = \frac{\text{number of data points}}{\text{number of internal knot spans}} = \frac{m+1}{n-p+1}$$

Then, define internal knots as,

$i = int(jt)$ where i is the largest integer s.t. $i \leq t$

$$\alpha = jt - i$$

$$u_{p+j} = (1-\alpha)\overline{u}_{i-1} + \alpha\overline{u}_i \tag{9}$$

Equation 9 guarantees that every knot span contains at least one $\overline{u}_k$. In such cases, the least squares approximation matrix (discussed in next section), $(N^T N)$ will be positive definite and well conditioned[3].

3.2.3 Solve for Unknown Control Points

There are two ways to solve for unknown control points that satisfy the error criterion:

- We can start with few control points, fit the curve, check for error, and add control points if necessary
- Start with many control points, fit the curve, check for error, and discard control points if possible

In our implementation, we start with few control points and a mean square error tolerance. We set the first and last control points to coincide with the data points:$\mathbf{Q}_0 = \mathbf{C}(0) = \mathbf{P}_0, \mathbf{Q}_m = \mathbf{C}(1) = \mathbf{P}_n$. Remaining $(m-1)$ data points are approximated in the least square sense, i.e, $\sum_{k=1}^{m-1} |\mathbf{Q}_k - \mathbf{C}(\overline{u}_k)|^2$ is a minimum with respect to $(n+1)$ control points, $\mathbf{P}_i$. In matrix form, this leads to a system of $(n-1)$ equations in $(n-1)$ unknowns,

$$(N^T N)\mathbf{P} = \mathbf{R} \tag{10}$$

where, N is the $(m-1) \times (n-1))$ matrix of scalars

$$N = \begin{bmatrix} N_{1,p}(\overline{u}_1) & \cdots & N_{n-1,p}(\overline{u}_1) \\ \vdots & \ddots & \vdots \\ N_{1,p}(\overline{u}_{m-1}) & \cdots & N_{n-1,p}(\overline{u}_{m-1}) \end{bmatrix}$$

R is the vector of $(n-1)$ points,

$$R = \begin{bmatrix} N_{1,p}(\overline{u}_1)\mathbf{R}_1 + \ldots + N_{1,p}(\overline{u}_{m-1})\mathbf{R}_{m-1} \\ \vdots \\ N_{n-1,p}(\overline{u}_1)\mathbf{R}_1 + \ldots + N_{n-1,p}(\overline{u}_{m-1})\mathbf{R}_{m-1} \end{bmatrix}$$

and $\mathbf{P}$ is a vector of control points.

$$\mathbf{P} = \begin{bmatrix} \mathbf{P}_1 \\ \vdots \\ \mathbf{P}_{n-1} \end{bmatrix}$$

Depending on the dimensionality of $\mathbf{P}_i$ (in our case, $\mathbf{P}_i$ are 3D (x, y, z) spatial points), we need to solve the matrix equation(10) for each of the coordinates (x, y *and* z).

3.2.4 NURBS Surface Lofting

Let $\{\mathbf{C}_k(\overline{u})\}$, $k = 0, \cdots, K$ be a set of curves that need to be lofted to form a NURBS surface. $\{\mathbf{C}_k(\overline{u})\}$ are planar sectional curves defined along a parametric direction, u. The curves may or may not have same parameterization, degree or knot vectors. Lofting[10] is a method of blending the sectional curves is an orthogonal parametric direction, v, through interpolation. The steps involved in lofting a surface are:

1. Choose a degree, p^*, usually highest of the degree of $\{\mathbf{C}_k(\overline{u})\}$
2. Raise each of $\{\mathbf{C}_k(\overline{u})\}$ to degree, p^*, using degree elevation
3. Redefine, if necessary, each of the $\{\mathbf{C}_k(\overline{u})\}$ on a common knot vector $\mathbf{U}^*$, using knot manipulation
4. Choose a degree, $q(q \leq K)$, parametric variables $\{v_k\}$, $k = 0, \cdots, K$, and compute a knot vector, $\mathbf{V}$, for the orthogonal parametric direction, v

5. Do $(n+1)$ curve interpolations across the control points of $\{\mathbf{C}_k(\overline{u})\}$ to obtain control points, $\mathbf{Q}_{i,j}(u,v)$ of the lofted surface

The parametric variables, $\{\overline{v}_k\}$ are computed as,

$$\overline{v}_k = \overline{v}_{k+1} + \frac{1}{n+1}\sum_{i=0}^{n}\frac{|\mathbf{P}_{i,k} - \mathbf{P}_{i,k-1}|}{d_i} \qquad k = 1, \cdots, K-1$$

4. MATERIALS AND METHODS

4.1 Image Data

A group of 12 subjects were imaged consisting of 5 normal volunteers (NRM), 3 patients with mitral regurgitation (MRR) and 4 patients with pulmonary hypertension (PHTN). All participants underwent MRI on a 1.5T MRI scanner (GE, Milwaukee, WI) optimized for cardiac application. Both cine and tagged images were acquired in standard views (2 and 4 chamber long axis and short axis) with a fast gradient echo cine sequence with the following parameters: FOV = 300 mm, image matrix = 256x256, flip angle = 45, TE = 1.82ms, TR = 5.2ms, number of cardiac phases = 20, slice thickness = 8 mm. A 2D spatial modulation of magnetization tagging preparation was done with a tag spacing of 7 pixels.

4.2 Model Fitting

Our algorithm has been tested for each of the patient data categories: normal subjects, patients with mitral regurgitation and pulmonary hypertension. Model fitting can be done for each of the desired anatomical part separately. Also, we can reconstruct combined bi-ventricular models. We illustrate reconstruction of heart anatomical models with several examples.

A very important advantage of our algorithm is accurate visualization of tag tracking errors across slices. In a typical study, we need to ensure accurate tracking of approximately, 170 tag lines (assuming 7 slices and 6 tag lines in each directions, two cardiac phases). Checking for proper tracking of each tag line is cumbersome and time consuming. Hence, our method fills the void of a good visualization and tag error identification program, that can be highly beneficial to an image analyst. Moreover, with the help of tag data visualization tool, we can get a snapshot of systolic (complete contraction) cardiac function like twisting and shortening of the left ventricle. We show several examples of reconstructed tag surfaces and tag tracking errors.

4.2.1 Left Ventricle

Contours were manually drawn on the images and NURBS curves of order=3 were fit to contours. The curve fitting error was less than 1 pixel. The NURBS curves were lofted setting order=3 in the orthogonal direction.

Many important indicators of cardiac health can be inferred from an analysis of LV endocardium. The endocardial model of LV for a normal control obtained from this method is illustrated in the figure (3).

The full surface model of left ventricle of a normal heart is shown in (Fig.4).

4.2.2 Right Ventricle

Using the method described in Section(4.2.1), we obtained NURBS model of the right ventricle as shown in Figure (5).

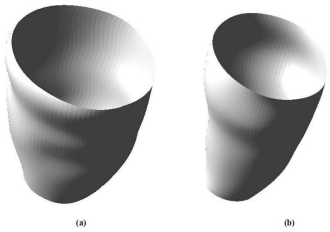

Figure 3: LV Endocardial Model. (a) End-Diastole. (b) End-Systole

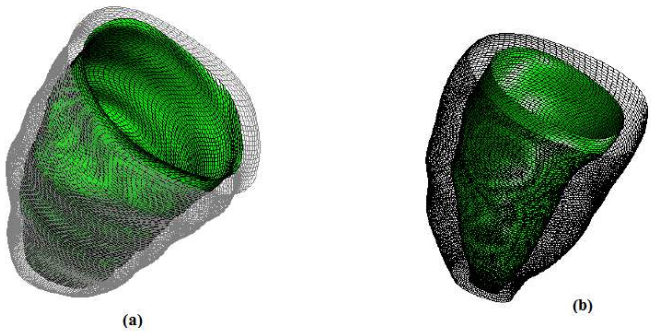

Figure 4: LV Endo- and Epi-Cardial Model. (a) End-Diastole. (b)End-Systole

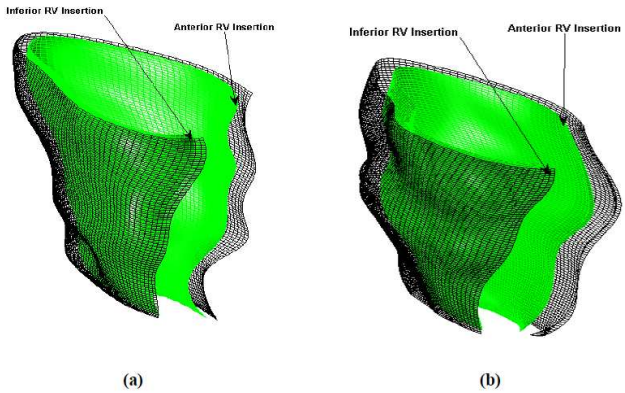

Figure 5: RV Models. (a) End-Diastole. (b) End-Systole

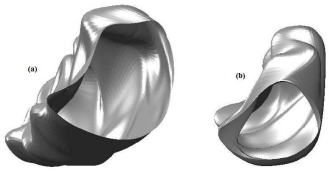

Figure 6: Endocardial surfaces of right ventricle of a patient suffering with pulmonary hypertension. (a)End-Diastole. (b)End-Systole

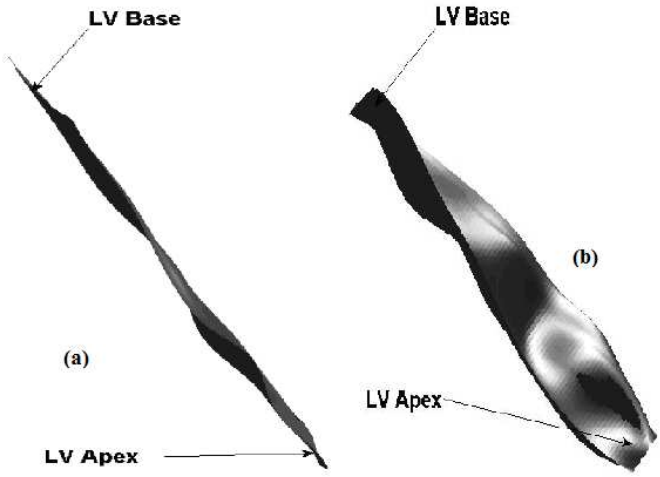

Figure 7: A single tag plane lofted showing tag plane twist and longitudinal shortening in LV. (a) End-Diastole. (b) End-Systole.

The method is effective in producing accurate models of pathological anatomies with irregular ventricular geometries as well. One such RV endocardial surface of a patient with severe pulmonary hypertension is illustrated in Fig.(6)

All NURBS models are fit in scanner coordinates obtained from DICOM header of MRI data. Actual anatomical dimensions are obtained from voxel dimensions. Hence, all models represent the true anatomical sizes and material point correspondence between model and actual tissue is always maintained.

4.2.3 Tag Surface Reconstruction

Tag detection and tracking was done semi-automatically using a method based on maximum likelihood/ maximum *a posteriori* (ML/MAP) framework[4]. Wrongly tracked tags were manually corrected and NURBS curves of order=3 were fit to each of the tracked tag lines. We lofted the tag surface across all slices for each tag index for short-axis images. Material point correspondence is ascertained by converting the pixel points to material points in scanner co-ordinates.

Figure 7 shows the tag surface lofted for one of the tag planes in end-diastole (ED) and end-systole (ES) phases. Longitudinal shortening and twisting of the tag plane in ES phase can be clearly observed.

Tag tracking algorithms can produce incorrect tracking results due to noise or large motion of the left ventricle. Two-dimensional tag tracking algorithms track a 3D tag plane as

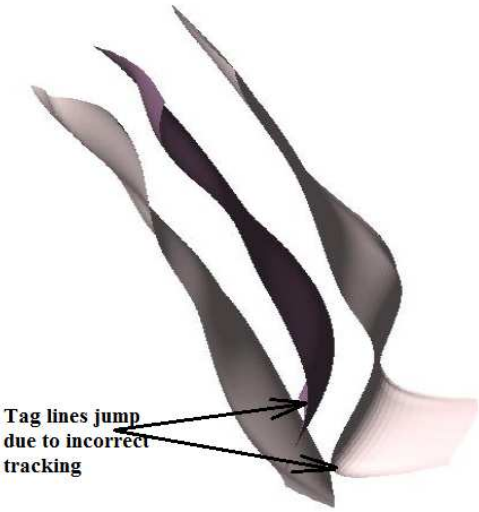

Figure 8: Visualization of incorrectly tracked tag lines(planes)

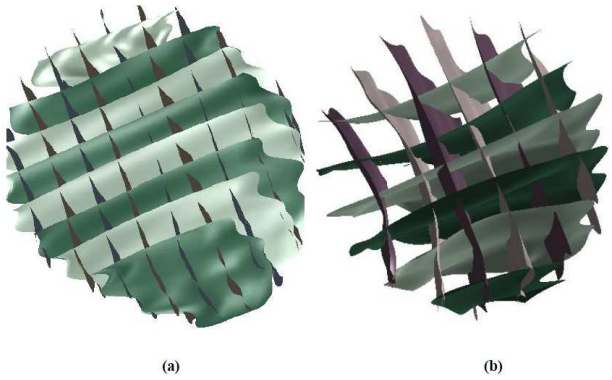

Figure 9: Reconstruction and visualization of tag data for a normal LV. (a)ED. (b)ES

multiple, independent 2D tag lines on different slices. This is because, the projections of a 3D tag plane on different imaging planes (slices) appear as lines. Due to different velocities at different slices, the tracking algorithm wrongly *"assigns"* a tag line to some other tag plane, to which, it does not belong. This is usually referred as, *"tag jumping"*. When a tag plane is lofted from its set of tag lines, an abnormal looking surface will result, if there is *tag jumping*. An illustration is in Figure(8).

Figure (9) illustrates accurate, anatomically correct reconstruction of all tag surfaces for the left ventricle.

We illustrate the complete biventricular model with reconstructed tag surfaces (LV and RV) incorporated into the myocardial surface model for a pathological heart with severe pulmonary hypertension (PHTN) in Figure(10).

5. DISCUSSION

All the myocardial models with the tag planes were reconstructed in scanner co-ordinates. Pixel points were converted to scanner co-ordinates using pixel spacing, *Image Position Patient* and *Image Orientation Patient* informa-

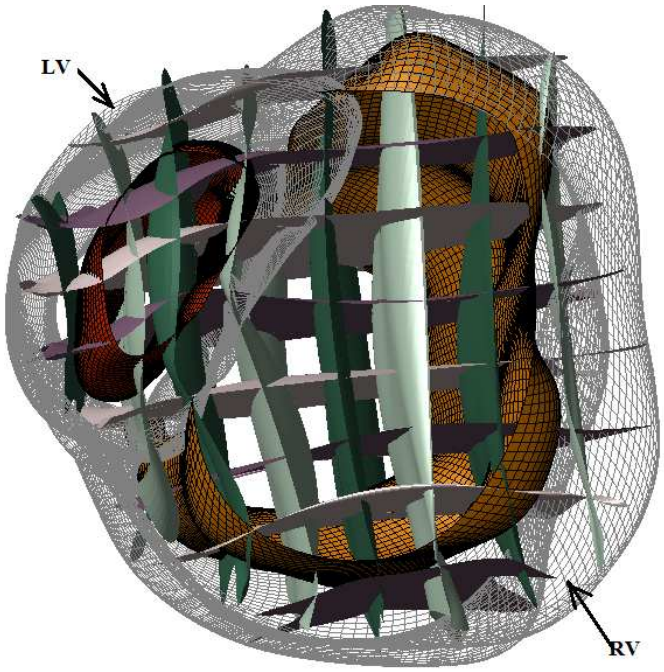

Figure 10: Full 3D model with LV and RV myocardial surfaces and tag planes

tion obtained from the DICOM header. Material point correspondence is established this way; hence models represent the actual object dimensions. The advantage of having material point correspondence is that the models can be used in computing classical descriptors of cardiac function like *Left Ventricular Volume (LVV)*, *Left Ventricular Mass (LVM)*, *Stroke Volume (SV)*, *Ejection Fraction (EF)* and *Cardiac Output (CO)*. Rational B-splines of order 4 (degree=3) were used for each parametric direction. Moreover, the user can choose any desired order of the curves and surfaces for model fitting, not necessarily order=4. The number of control points range anywhere from 20×10 to 300×10, depending on the complexity of the ventricular and tag surface geometry. If desired, the user can use fixed number of control points for desired accuracy and speed. For a complete study, computing the full model took less than 30 seconds on a PC with Intel® Core™ 2 Duo Processor (2.66 G Hz) with 3GB memory, after manual contouring and semi-automated tag tracking. The surfaces are uncoupled and we hypothesize uncoupling will be useful in overcoming the folding problem associated with nonrigid registration.

6. CONCLUSION

Our 3-D NURBS models can accurately model the myocardial (LV/RV) surfaces and tag data. The models can be extended to 4-D. The models will be helpful in evaluating the effectiveness of tag tracking algorithms and visualization. The proposed method allows us to recover the exact geometry of myocardial surfaces and tag planes. The method also allows for NURBS surfaces to be stored effectively with less memory and perform various tasks like shape analysis and query based model retrieval. The method can also be applied to CT, PET, SPECT or any other tomographic imaging modality for surface reconstruction from multiple cross sections. Another possible application of the models is in building pathology specific biventricular phantoms[14] (computer patients) for evaluation of novel imaging systems and image analysis algorithms.

7. REFERENCES

[1] L. Axel and L. Dougherty. MR imaging of motion with spatial modulation of magnetization. *Radiology*, 171(3):841–45, August 1989.

[2] J. Cauvin, J. Boire, M. Zanca, J. Bonny, J. Maublant, and A. Veyre. 3D modeling in myocardial 201tl SPECT. *Comput. Med. Imag. Graph.*, 17(4–5):345–350, 1993.

[3] C. deBoor. *A Practical Guide to Splines*. Springer-Verlag, 1978.

[4] T. Denney. Estimation and detection of myocardial tags in MR image without user-defined myocardial contours. *IEEE Transactions on Medical Imaging*, 18(4):330–334, 1999.

[5] J. Duncan, P. Shi, T. Constable, and A. Sinusas. Physical and geometrical modeling for image-based recovery of left ventricular deformation. *Progress in Biophysics and Molecular Biology*, 69(2–3):333–351, 1998.

[6] E. Haber, D. Metaxas, and L. Axel. Three-dimensional geometric modeling of cardiac right and left ventricles. In *The Biomedical Engineering Society Annual Meeting*, San Diego.

[7] M. Kuwahara and S. Eiho. 3-D heart image reconstruction from MRI data. *Computerized Medical Imaging and Graphics*, 15(4):241–246, 1991.

[8] J. Maehle, K. Bjoernstad, S. Aakhus, H. Torp, and B. Angelsen. Three-dimensional echocardiography for quantitative left ventricular wall motion analysis: A method for reconstruction of endocardial surface and evaluation of regional dysfunction. *Echocardiography*, 11(4):397–408, 1994.

[9] D. Metaxas and D. Terzopoulos. Shape and nonrigid motion estimation through physiscs-based synthesis. *IEEE Transactions on Pattern Analysis and Machine Intelligence*, 15(6):580, 1993.

[10] L. Piegl and W. Tiller. *The NURBS Book*. Springer-Verlag, 1997.

[11] P. Radeva, A. Amini, and J. Huang. Deformable b-solids and implicit snakes for 3-D localization and tracking of SPAMM-MRI data. *Computer Vision and Image Understanding*, 66(2):163–178, 1997.

[12] P. Shi, A. Sinusas, R. Constable, E. Ritman, and J. Duncan. Point-tracked quantitative analysis of left ventricle surface from 3d image sequences: Algorithms and validation. *IEEE Transactions of Medical Imaging*, 19(1):36–50, 2000.

[13] N. Tustison and A. Amini. Biventricular myocardial strains via nonrigid registration of anatomical models. *IEEE Transactions on Medical Imaging*, 25(1):94–112, 2006.

[14] A. Veress, W. Segars, B. Tsui, J. Weiss, and G. Gullberg. Normal and pathological NCAT image and phantom data based on physiologically realistic left ventricle finite element models. *IEEE Transactions on Medical Imaging*, 25(12):1604–16, December 2006.

[15] E. Zerhouni, D. Parish, W. Rogers, A. Yang, and E. Shapiro. Human heart: Tagging with MR imaging - a method for noninvasive assessment of myocardial motion. *Radiology*, 169(1):59–63, October 1988.